Propagation of invasive plant species in the presence of a road.

Deeley, Bradly; Petrovskaya, Natalia

DOI:
10.1016/j.jtbi.2022.111196

Document Version
Publisher's PDF, also known as Version of record

Citation for published version (Harvard):
Deeley, B & Petrovskaya, N 2022, 'Propagation of invasive plant species in the presence of a road.', *Journal of Theoretical Biology*, vol. 548, 111196. https://doi.org/10.1016/j.jtbi.2022.111196

Journal of Theoretical Biology 548 (2022) 111196

Contents lists available at ScienceDirect

Journal of Theoretical Biology

journal homepage: www.elsevier.com/locate/yjtbi

Propagation of invasive plant species in the presence of a road

Bradly Deeley, Natalia Petrovskaya *

School of Mathematics, University of Birmingham, Birmingham, UK

ARTICLE INFO

Article history:
Received 31 December 2021
Revised 3 May 2022
Accepted 7 June 2022
Available online 16 June 2022

Keywords:
Invasive plants
Fragmented landscape
Logistic growth
Allee effect
Dispersal kernel
Integro-difference equation

ABSTRACT

Invasive plant species pose a significant threat to biodiversity and the economy, yet their management is often resource-intensive and expensive, and further research is required to make control measures more efficient. Evidence suggests that roads can have an important effect on the spread of invasive plant species, although little is known about the underlying mechanisms at play. We have developed a novel mathematical model to analyse the impact of roads on the propagation of invasive plants. The integro-difference equation model is formulated for stage-structured population and incorporates a road subdomain in the spatial domain. The results of our study reveal, that, depending on the definition of the growth function in the model, there are three distinct types of behaviour in front of the road. Roads can act as barriers to invasion, lead to a formation of a beachhead in front of the road, or act as corridors allowing the invasive species to invade the domain in front of the road. Analytical and computational findings on how roads can impact the spread of invasive species show that a small change in conditions of the environment favouring the invasive species can change the case for the road, allowing the invasive species to invade the domain in front of the road where it previously could not spread.

1. Introduction

Biological invasion is identified as one of the most serious environmental problems currently facing society. Invasion of plant species in various habitats across the world cause the damage to both the ecosystem and economy, the losses being evaluated as billions of dollars each year (Pimentel et al., 2000), at an increasing rate (Sala et al., 2000).

The conditions for propagation of invasive species are different in different landscapes and the influence of the surrounding landscape on the spread dynamics of invasive plants has been well recognised (O'Reilly-Nugent et al., 2016; Vilà, 2011). Among other important habitats, the problem of invasion of alien plants in forests has received a lot of attention (e.g., see Essl et al., 2011; Langmaier and Lapin, 2020; Sanderson et al., 2012). Invasive plant species pose a significant threat to biodiversity in native forest areas, yet their management is resource-intensive and expensive. Any action to prevent or mitigate the consequences of biological invasion in the forest is important as the environment and economy suffer from huge losses related to the spread of invasive species into native forest areas (Holmes et al., 2009).

Forest roads are nowadays an essential part of the landscape and they can play an important role in the spread of invasive plant species. It has been debated that roads can serve as transport corridors for movement as well as providing prime habitat for establishment of invasive plants (Forman et al., 2002; Mortensen et al., 2009; Tyser and Worley, 1992). However, the role of forest roads as transport corridors for invasive plants is not completely understood. Although it has been widely studied (Damschen et al., 2014; Nathan et al., 2011) to what effect corridors increase the movement of species, this debate is still ongoing (Travers et al., 2021) and much of this work has been done from the view point of conservation of species and connecting fragmented landscapes to increase the chances of success of a given species (cf. Gilbert-Norton et al., 2010; Haddad et al., 2003). Furthermore, the evidence that roads facilitate plant invasion is controversial, and the study in Hansen and Clevenger (2005) has shown that not all ecosystems close to roads are invaded to the same extent.

In our paper, a mathematical and computational model of biological invasion in the heterogeneous landscape has been developed to predict how invasive plants will be spreading when the forest area is fragmented by building a road. The model parameters are determined to simulate the spatio-temporal dynamics of the invasive plant and find threshold values responsible for spread when a new landscape feature (a road) is introduced. It will be shown in the paper that growth is a key factor determining the propagation of the invasive species. Analysing both logistic and Allee growth functions, our analytical and computational findings on how roads can impact the spread of invasive species

* Corresponding author.
E-mail address: n.b.petrovskaya@bham.ac.uk (N. Petrovskaya).

https://doi.org/10.1016/j.jtbi.2022.111196
0022-5193/

demonstrate that there are several distinct types of behaviour in front of the road.

The paper is organized as follows. In the next section, we first formulate a mathematical model of biological invasion used to simulate spatio-temporal dynamics of the invasive species. The model is stage-structured, where the reproduction and dispersal stage are considered independently at each discrete time step, and the dispersal stage is modelled by an integro-difference equation. We then explain in Section 2.2 how the model is modified to include a road environment into it. In Section 3, we compare propagation of the invasive plant species when its growth is controlled by either the logistic growth function (Section 3.1) or the growth function with the Allee effect (Section 3.2). It will be argued in the paper that the road model with the logistic growth function has two basic scenarios of propagation of the invasive species: the 'corridor' regime and the 'barrier' regime. In the latter case, the road prevents invasion completely, while in the former case, the invasive species invades the domain in front of the road. The spatio-temporal population dynamics observed in the 'road' model is more complicated when the Allee effect is taken into account in the definition of the growth function. In the case of the Allee growth function, a new propagation regime labelled 'beachhead' appears, and we perform analytical and computational study of the beachhead regime in Section 3.2. While our present study is restricted by a $1-D$ spatial layout, the extension of our results onto a $2-D$ system is briefly discussed in Section 4, where concluding remarks are provided.

2. The model

2.1. The 'no road' model

We consider an invasive species described by its population density N, where we assume that the life cycle of the invasive species exhibits two distinctly different stages. The first one is the demographic stage which can include the growth of juveniles, their maturation, mating and reproduction, while the second stage is dispersal. We are mainly interested in modeling invasive plant species, and many plant species reproduce at certain time intervals throughout the year, for example on a yearly cycle through seed dispersal or pollination (Lewis et al., 2016).

The above biological settings are best taken into account by a discrete time framework (Kot and Schaffer, 1986) where the population density evolves from generation t to generation $t+1$, i.e. we consider the discrete time with the increment $\delta t = 1$. Let $N(t,x) \equiv N_t(x)$ be the population density in generation t over continuous space x. For convenience of interpretation only, we assume that the species first goes through the demographic stage and will then disperse. The demographic stage is described as

$$\widetilde{N}_t(x) = F(N_t(x)), \tag{1}$$

where $N_t(x)$ is the species' spatial distribution emerging after the dispersal stage in the previous generation, and $F(N_t)$ is the growth function.

In our study, we consider two growth functions. The logistic growth of the population density N is given by

$$F(N) = AN\exp(-N), \tag{2}$$

where the growth parameter is $A > 0$. The steady states $\bar{N}$ of a non-spatial problem that corresponds to the demographic stage (1) are given by

$$\bar{N}_{t+1} = F(\bar{N}_t), \tag{3}$$

where, apart from the trivial solution $\bar{N}_1 = 0$, we have a locally stable steady state

$$\bar{N}_2 = ln(A), \tag{4}$$

for the logistic growth function (2).

We also consider an example of the growth function with Allee effect taken from Boukal and Berec (2002),

$$F(N) = \frac{\rho N^2}{A+N^2}, \tag{5}$$

where $A > 0$ and $\rho > 0$. The non-convex shape of the function (5) means that the population growth is affected by a strong Allee effect as the population declines at low densities. The non-spatial problem (3) has a single equilibrium solution at $\bar{N}_1 = 0$ when $\rho < 2\sqrt{A}$ (unconditional extinction regime), and there is extinction-survival behaviour of the population $N(t)$ in (3), when $\rho \geqslant 2\sqrt{A}$. A straight line

$$\rho = 2\sqrt{A} \tag{6}$$

is a boundary between the two regimes in the parametric plane (A,ρ). In the extinction-survival case we have the following steady state solutions

$$\bar{N}_1 = 0, \bar{N}_2 = \frac{\rho - \sqrt{\rho^2 - 4A}}{2}, \bar{N}_3 = \frac{\rho + \sqrt{\rho^2 - 4A}}{2}, \tag{7}$$

where $\bar{N}_2 = \bar{N}_3 = \frac{\rho}{2}$ when $\rho = 2\sqrt{A}$. The non-trivial steady state solution $\bar{N}_2$ is locally unstable, while $\bar{N}_3$ is a stable solution.

After the demographic stage of the given generation is complete, the species enter the dispersal stage, which when finished, produces the species' spatial distribution in the next generation:

$$N_{t+1}(x) = \int_\Omega \widetilde{N}_t(y)k(x,y)dy, \tag{8}$$

where Ω is a dispersal domain whose definition is discussed later. The dispersal kernel $k(x,y)$ in (8) is the probability density function of the event that an individual moves from position y to position x after dispersal. The dispersal kernel satisfies

$$\int_\Omega k(x,y)\,dx = \int_\Omega k(x,y)\,dy \equiv 1. \tag{9}$$

In this paper, we consider the Gaussian dispersal kernel given by

$$k(x,y) = \frac{1}{\sqrt{2\pi\sigma^2}}\exp\left(-\frac{|x-y|^2}{2\sigma^2}\right), \tag{10}$$

where the standard deviation σ is the parameter quantifying the spatial scale of the dispersal (but see, *e.g.*, Andersen, 1991 for further discussion of the choice of a dispersal kernel).

Having substituted (1) into (8), we exclude the variable $\widetilde{N}_t$ and obtain the following integro-difference equation for the population density in generation $t+1$:

$$N_{t+1}(x) = \int_\Omega F(N_t(y))k(x,y)\,dy. \tag{11}$$

We use the following initial condition to simulate the spatial distribution $N_0(x)$ of an invading population:

$$N_0(x) = \frac{1}{\sqrt{2\pi}}\exp\left(-\frac{x^2}{2}\right). \tag{12}$$

The integro-difference Eq. (11), along with the definition of the growth function (2) or (5) and the initial condition (12), is solved numerically in a spatial domain $\Omega = \{x : -L \leqslant x \leqslant L\}$. The fast Fourier transform method is used to obtain the population density distribution at time $t+1$; see Rodrigues et al. (2015) for further explanation of the numerical method. We note that, since the dispersal kernel (10) is positive over the whole space, the population

density in (11) is positive everywhere in space at any time $t > 0$. However, very small densities are not biologically feasible and therefore we apply an additional restriction on the population density in our numerical solution:

$$N_{t+1}(x) = \begin{cases} 0, & \text{if } \widehat{N}_{t+1}(x) < \epsilon, \\ \widehat{N}_{t+1}(x), & \text{otherwise}, \end{cases} \tag{13}$$

where ϵ is a selected small threshold value of the population density.

Numerical solution of the integro-difference Eq. (11) requires that the domain size L is large enough to provide an accurate approximation of the solution in a finite spatial domain. In other words, the numerical solution should not be sensitive to the conditions at the domain boundaries, should any boundary condition be required (Rodrigues et al., 2015). If L is chosen to be insufficiently large, then 'boundary forcing' may occur, and the population dynamics inside the domain may be affected by the boundary conditions[1]. For the rest of this paper, we assume that the domain size L is large enough to provide a correct numerical solution $N_{t+1}(x)$ for any time $t+1$ we are interested in.

2.2. The 'road' model

A generic model (11)–(12) introduced in the previous section is referred to as the 'baseline' or 'no road' model further in the text. We now expand the no road model to include the 'road' environment into it where we assume that the growth and dispersal conditions are different in the 'road' spatial sub-domain (cf. Musgrave et al., 2015). Consider a road subdomain $\Omega_R \subset \Omega$ and let us introduce an additional dispersal stage over the road in our model as the discrete time progresses from t to $t+1$. This is done by splitting the time interval from t to $t+1$ into two subintervals. We first consider the no road case (11), but treat the solution as obtained at time $t+\frac{1}{2}$, i.e., we have:

$$N_{t+\frac{1}{2}}(x) = \int_{-L}^{L} F(N_t(y))k(x,y)\,dy. \tag{14}$$

Next, we identify the population density N^R for the region of the road, where additional dispersal will happen

$$N^R_{t+\frac{1}{2}}(x) = \begin{cases} N_{t+\frac{1}{2}}(x), & \text{if } x \in \Omega_R, \\ 0, & \text{otherwise}. \end{cases} \tag{15}$$

We now apply an additional dispersal step to the road based on the assumption that the population (e.g., seeds of an invasive plant) cannot grow on the road and is taken away from the road quickly (e.g., by the wind). We have

$$N^R_{t+1}(x) = \int_{-L}^{L} N^R_{t+\frac{1}{2}}(y)k(x,y)\,dy. \tag{16}$$

This additional dispersal that moves the population away from the road contributes to the population density distribution at time $t+1$ as follows

$$\widehat{N}_{t+1}(x) = N_{t+\frac{1}{2}}(x) + N^R_{t+1}(x),\ x \in \Omega. \tag{17}$$

Finally, we assume that the population we have across the road after the additional dispersal step (16) dies out, i.e., we modify the condition (13) as follows

$$N_{t+1}(x) = \begin{cases} 0, & \text{if } x \in \Omega_R, \text{ or if } \widehat{N}_{t+1}(x) < \epsilon, \\ \widehat{N}_{t+1}(x), & \text{otherwise}, \end{cases} \tag{18}$$

obtaining the population density distribution over the domain Ω at time $t+1$. We will refer to the model (14)-(18) as the 'road' model further in the text.

3. Results: comparison of the no road model and the road model

For the sake of further discussion, we first briefly present the results of the simulation in the no road model before we introduce the road layout. For the rest of this paper, we set up $\sigma = 0.1$ in the dispersal kernel (10) (unless it is explicitly defined) and the domain length is always chosen as $L = 10$. The threshold density is $\epsilon = 10^{-7}$ in all computations.

The no road model (11)–(12) is well studied (*e.g.,* see Kot et al., 1996), and it is known that the invasive species will spread as a travelling wave over the domain at a constant rate as time progresses. An example of propagation of the invasive species into the space is shown in Fig. 1, where the logistic growth function (2) has been used in simulation, and the height h of the travelling wave is therefore defined from (4) as $h = ln(A)$. Spatial distributions of the population density observed for the growth function with the Allee effect are topologically very similar to those in Fig. 1, and we do not show them here.

The constant spread rate of the travelling wave can be evaluated based on linearisation of the growth function, *e.g.,* see Lewis et al., 2016. For the logistic growth function (2), we have

$$c_{theor} = \sqrt{2\sigma^2 ln(A)}. \tag{19}$$

In our numerical experiments, we have seen a good agreement with the theoretical result (19) and the spread rate c computed directly from the numerical solution. In the latter case we have identified the front position x^f of the travelling wave at two consecutive moments of time t and $t+1$ to compute

$$c = x^f(t+1) - x^f(t). \tag{20}$$

Given values c_{theor} and c, a difference between them has been $|c_{theor} - c| \approx 10^{-3}$. A very small discrepancy between c_{theor} and c confirms the accuracy of our numerical method to make sure that the numerical results are free of any artifacts when computation is made for a more numerically advanced road model.

Next, we consider the road problem (14)-(18). Unlike the no road case, the spatio-temporal dynamics are different when different growth functions are employed in the problem. We first discuss a simpler case of the logistic growth function (2).

3.1. The road model with the logistic growth function

Depending on the road width, there are two basic scenarios of wave propagation that we label as the 'corridor' and 'barrier' regimes when the growth function (2) is used in the model. In the former case, the population would cross the road and subsequently go on to invade the whole domain. In the latter case, the road would act as a barrier to invasion and the invasive species cannot cross the road. The examples of wave propagation in the corridor and barrier cases are shown in Fig. 2 and Fig. 3, respectively.

It is clear from comparison of the spatio-temporal dynamics in Fig. 2 and Fig. 3 that a travelling wave passes through a narrow road region without any transformation, while a wide road prevents the population wave from further propagation entirely. Thus,

[1] For a detailed discussion of this issue see Rodrigues et al. (2015), where recommendations have also been given on the choice of L required to keep the solution error within the desired accuracy.

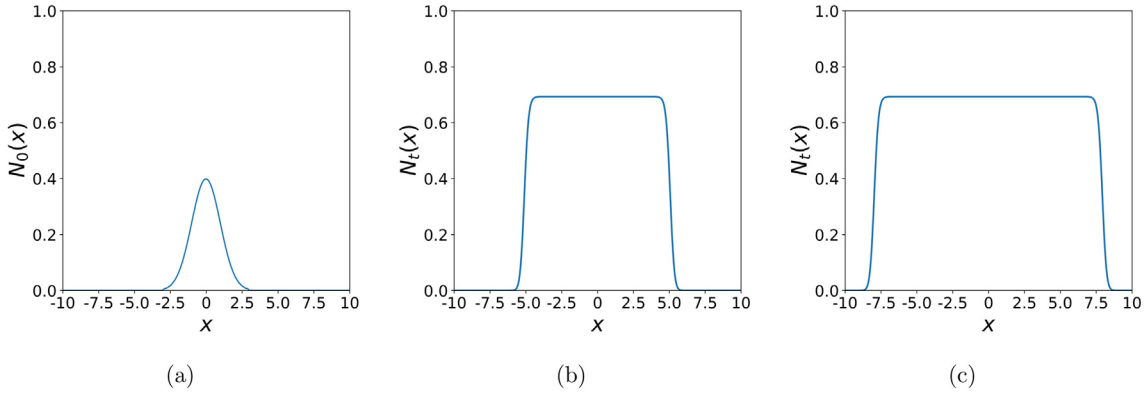

Fig. 1. The no road model: a travelling wave solution $N(x,t)$ for the problem (11)–(12) with the growth function (2). The parameters are $A = 2$ and $\sigma = 0.1$. (a) The initial distribution (12) at time $t = 0$, (b) The population density distribution $N_t(x)$ at time $t = 25$, (c) The invasive species spreads further into the space as time progresses, $t = 50$. Similar spatial distributions of the population density are observed when the growth function (5) is used in simulation.

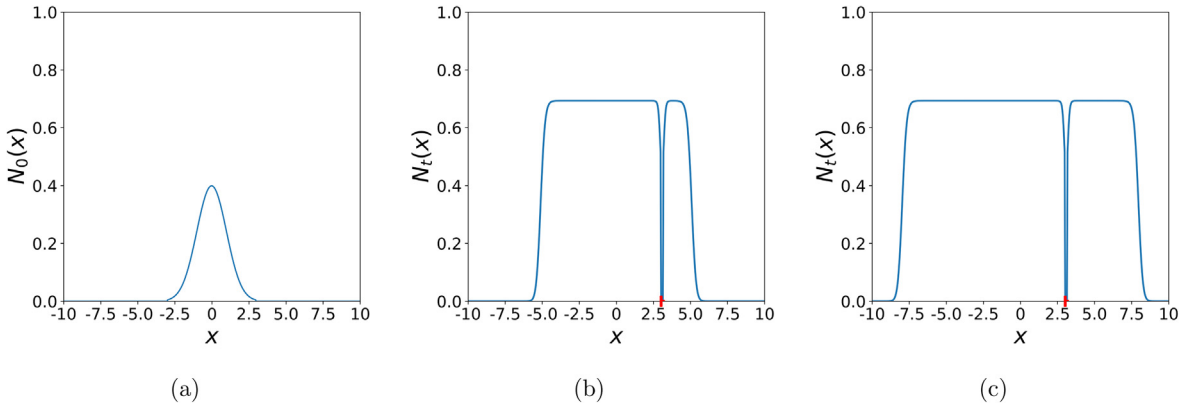

Fig. 2. The road model: spatio-temporal dynamics of the population density $N(x,t)$ in the problem (14)-(18) with the growth function (2), where $A = 2$. The road region is shown in red on the x-axis, where the road width $\delta = 0.12$ results in the corridor case. (a) The initial distribution (12) at time $t = 0$, (b) The population density distribution $N_t(x)$ at time $t = 25$, as the invasive species propagates in front of the road, (c) The invasive species spreads further into the space in front of the road as time progresses, $t = 50$.

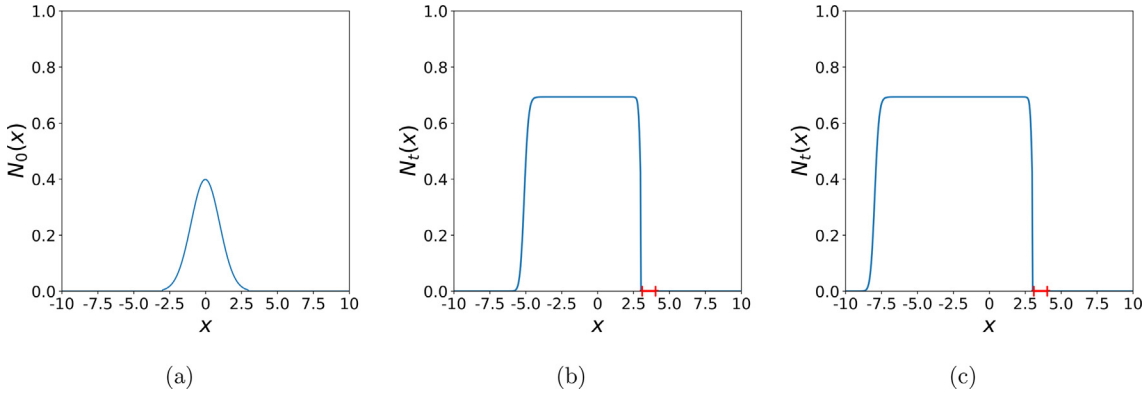

Fig. 3. The barrier regime in the problem (14)-(18) with the growth function (2). The road width is $\delta = 1.2$, the other parameters are the same as in Fig. 2. (a) The initial distribution (12) at time $t = 0$, (b) The population density distribution $N_t(x)$ at time $t = 25$: the invasive species approaches the road yet it does not cross the road and does not propagate in front of the road, (c) The invasive species can only propagate behind the road as time progresses, $t = 50$.

our next aim is to evaluate the critical width of the road where a transition between the corridor regime and barrier regime occurs for any given value of the growth parameter A in the function (2). Let us assume that the travelling wave approaches the road of width δ positioned at $\Omega_R = [b, b+\delta]$ from the left at time t (*e.g.*, see Fig. 3b). We approximate the population density in the travelling wave at time t as follows:

$$N_t(x) = \begin{cases} h, & \text{if } x \in [a,b], \\ 0, & \text{otherwise}, \end{cases} \tag{21}$$

where the height h of the wave is given by (4) for the growth function (2). The population density at time $t+1$ is given by

$$N_{t+1}(x) = N_{t+\frac{1}{2}}(x) + N^R_{t+1}(x), \tag{22}$$

where at the dispersal stage with the kernel (10) we have

$$\begin{aligned} N_{t+\frac{1}{2}}(x) &= \int_\Omega F(N_t(y))k(x,y)\,dy \\ &= F(h)\int_a^b \frac{1}{\sqrt{2\pi\sigma^2}}\exp\left(\frac{-|x-y|^2}{2\sigma^2}\right)dy \\ &= F(h)\frac{1}{2}\left(\operatorname{erf}\left(\frac{b-x}{\sigma\sqrt{2}}\right)+\operatorname{erf}\left(\frac{x-a}{\sigma\sqrt{2}}\right)\right). \end{aligned} \tag{23}$$

We now calculate the additional dispersal of the population density $N^R_{t+1}(x)$ across the road. According to (15) and (16) in the road model, we have

$$\begin{aligned} N^R_{t+1}(x) = F(h)\frac{1}{2}\int_b^{b+\delta}&\left(\operatorname{erf}\left(\frac{b-y}{\sigma\sqrt{2}}\right)+\operatorname{erf}\left(\frac{y-a}{\sigma\sqrt{2}}\right)\right) \\ &\times\left(\frac{1}{\sqrt{2\pi\sigma^2}}\exp\left(\frac{-|x-y|^2}{2\sigma^2}\right)\right)dy. \end{aligned} \tag{24}$$

We then use the approach in Tsay et al. (2013) to approximate the integral in (24). We have

$$\begin{aligned} N^R_{t+1}(x) = F(h)\frac{1}{2}\frac{1}{\sqrt{2\pi\sigma^2}}\int_b^{b+\delta}&\left(\exp(-d_1y^2+d_2y+d_3)\right. \\ &\left.-\exp(-d_1y^2+d_4y+d_5)\right)dy, \end{aligned} \tag{25}$$

where coefficients $d_i = d_i(x), i = 1,\dots,5$ are calculated in Appendix A. Substituting (23) and (25) into (22), integrating, and rearranging terms we arrive at

$$N_{t+1}(x) = F(h)\phi(x,\delta), \tag{26}$$

where the function $\phi(x,\delta)$ is given by

$$\begin{aligned} \phi(x,\delta) = \Bigg[&\frac{1}{4}\frac{1}{\sqrt{d_1}}\frac{1}{\sqrt{2\sigma^2}}\left(\exp\left(\frac{d_2^2}{4d_1}+d_3\right)\left(\operatorname{erf}\left(\frac{2d_1(b+\delta)-d_2}{2\sqrt{d_1}}\right)\right.\right. \\ &\left.+\operatorname{erf}\left(\frac{d_2-2d_1b}{2\sqrt{d_1}}\right)\right)-\exp\left(\frac{d_4^2}{4d_1}+d_5\right) \\ &\times\left(\operatorname{erf}\left(\frac{2d_1(b+\delta)-d_4}{2\sqrt{d_1}}\right)+\operatorname{erf}\left(\frac{d_4-2d_1b}{2\sqrt{d_1}}\right)\right)\Bigg) \\ &+\frac{1}{2}\left(\operatorname{erf}\left(\frac{b-x}{\sigma\sqrt{2}}\right)+\operatorname{erf}\left(\frac{x-a}{\sigma\sqrt{2}}\right)\right)\Bigg]. \end{aligned} \tag{27}$$

If the population density at time $t+1$ is $N_{t+1}(x) > \epsilon$ for $x \in [b+\delta, L]$, the population will grow in the spatial domain in front of the road, *i.e.,* we have the corridor regime as shown in Fig. 2. Thus, to find the boundary between the corridor and barrier case we have to solve

$$F(h)\phi(\delta) = \epsilon, \tag{28}$$

where the function ϕ defined by (27) is considered at the point $x = b+\delta$. We now require that $F(h) = h$, substitute $h = ln(A)$ into (28) and rearrange terms to arrive at

$$A = \exp\left(\frac{\epsilon}{\phi(\delta)}\right). \tag{29}$$

The expression (29) defines the boundary curve separating the barrier region from the corridor region in the (A,δ)-plane. For any given value of the demographic parameter A in the growth function (2), a critical road width δ_b required to prevent propagation of the invasive species in front of the road can be calculated from (29). We note that for the logistics growth function (2), we also have the boundary separating the extinction and survival regions. Hence, there are two boundary curves in the parametric plane (A,δ). The straight line $B_1 : A = 1$ is the boundary between the extinction and survival regions, while the boundary $B_2 : \delta_b = \delta_b(A)$ defined from solving (29) separates the corridor and the barrier regions; see Fig. 4.

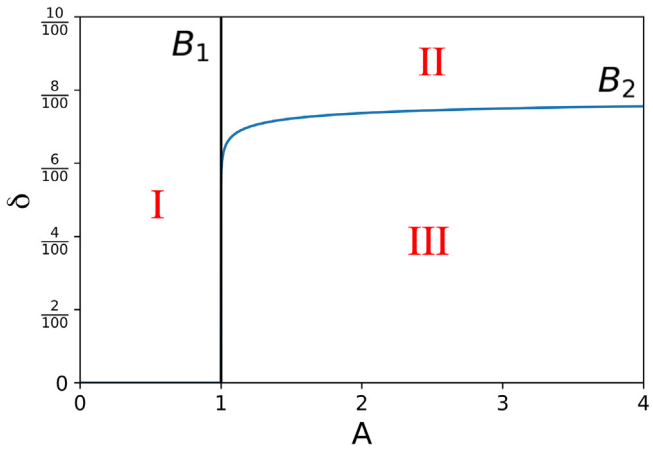

Fig. 4. Various propagation regimes in the road model (14)-(18) with the growth function (2). The road width δ is measured as a percentage of the domain size L. Region I in the parametric plane (A,δ) represents the extinction regime in the spatial domain, region II is the barrier regime, where the road prevents propagation of the invasive species, and region III is the corridor regime, where the invasive population crosses the road and a travelling wave spreads in front of the road. The boundary B_2 between regions II and III determines the critical width of the road required to stop propagation of the invasive species for a given value of the growth parameter A.

We want to emphasise here that the existence of the barrier regime in the problem is entirely due to the threshold density ϵ in (18). For any $A > 1$, the invasive species will always propagate when we have $\epsilon = 0$ in (28), no matter what the road width is. Consider now the case when ϵ increases, i.e., we have harsher growth conditions in front of the road. Let the original threshold density be $\epsilon = \epsilon^*$, and the new threshold density be $\epsilon^{**} > \epsilon^*$. Consider a point $P = (A, \delta_b^*)$ at the boundary B_2 obtained for the threshold ϵ^*. Given the same value of A, the position of P will change when the new value of ϵ^{**} is implemented in the problem. It follows from (29) that

$$A = \exp\left(\frac{\epsilon^*}{\phi(\delta_b^*)}\right) = \exp\left(\frac{\epsilon^{**}}{\phi(\delta_b^{**})}\right),$$

where δ_b^{**} is the road width for which $P = (A, \delta_b^{**}) \in B_2$ when $\epsilon = \epsilon^{**}$. Rearranging terms we obtain

$$\frac{\epsilon^{**}}{\epsilon^*} = \frac{\phi(\delta_b^{**})}{\phi(\delta_b^*)},$$

and, since $\epsilon^{**}/\epsilon^* > 1$, we have $\phi(\delta_b^{**}) > \phi(\delta_b^*)$.

The graph of the function $\phi(\delta)$ is shown in Fig. 5. It can be seen from the graph that $\phi(\delta)$ is a decreasing function of its argument and therefore $\delta_b^{**} < \delta_b^*$, *i.e.,* the point P moves down along the vertical axis in Fig. 4. Hence, if the threshold density ϵ increases, the boundary B_2 will go down in the parametric plane (A,δ) to increase the area of the barrier region. In other words, if environmental conditions become harsher in front of the road, a more narrow road can still prevent propagation of the invasive species. Conversely, for smaller values of ϵ, the boundary B_2 will go up to make the corridor regime region larger in the parametric plane.

Our previous investigation has been performed for the fixed value $\sigma = 0.1$ in the dispersal kernel (10). We now discuss briefly how the critical value δ_b of the road width responsible for the transition from the corridor regime to the barrier regime depends on the parameter σ in the dispersal kernel. Let us fix the parameters

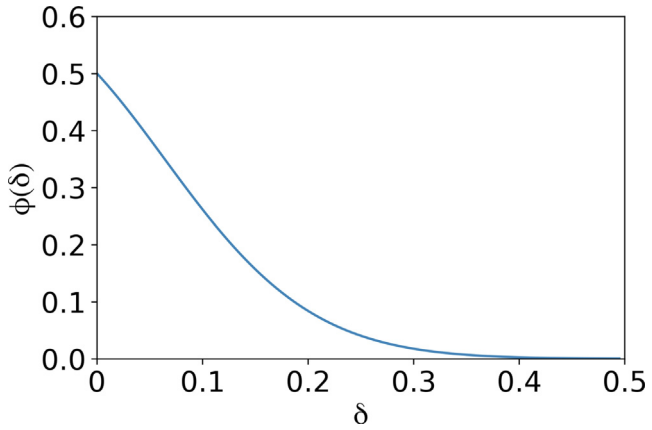

Fig. 5. The function $\phi(x,\delta)$ defined by (27) and considered at the right edge x_r of the road, $x_r = b+\delta$, is a decreasing function of the argument δ.

A and ϵ and vary σ in the Eq. (28). The function ϕ defined by (27) at the point $x = b+\delta$ becomes a function of variables σ and δ only, and the Eq. (28) can be solved to obtain the curve $B_\sigma : \delta = \delta(\sigma)$ defining the boundary between the corridor and barrier regime.

The boundary curve B_σ is shown in Fig. 6a. We note that a semi-analytical approach used to obtain the curve B_σ as explained above does not require any upper bound for variables δ and σ in the definition of the function ϕ in (27). However, the choice of the large parameter $\sigma \gg 1$ results in a degenerate dispersal kernel, *i.e.,* the dispersal is so weak that any road width can be considered as a barrier; see Fig. 6a. Hence, we also show a fragment of the boundary curve B_σ obtained for small σ in Fig. 6b. It can be seen from the figure that an increase in σ within the interval $\sigma \in [0,1]$ results in a linear growth of the corridor domain, *i.e.,* we have $\delta = \kappa\sigma$, where the slope κ of a straight line in the figure can be approximated as $\kappa \approx 7.38$ for $\epsilon = 10^{-7}$ and $A = 3$ used in computation.

3.2. The road model with the Allee effect growth function

The spatio-temporal population dynamics observed in the road model is more complicated when the Allee effect is taken into account in the definition of the growth function. We still have the corridor and barrier regimes when the growth function (5) is used in the model. Wave patterns of the population density observed for those regimes are very similar to those presented in Fig. 2 (the corridor case) and Fig. 3 (the barrier case), and we do not show them here. Meanwhile, for the growth function (5), there exists the range of the road width $\delta \in [\delta_1, \delta_2]$ where we observe a new regime in the spatio-temporal dynamics of the invasive species. One example of this new regime labelled as 'beachhead' in the model is shown in Fig. 7. It can be seen from the figure that, while a spatial region in front of the road has been invaded, the population in front of the road does not propagate further into the space as time progresses.

The existence of the beachhead regime for the growth function (5) is further illustrated by results in Fig. 8, where we show the rate of spread c and the width W of a domain occupied by the population in front of the road as functions of the road width δ. It is seen from the simultaneous analysis of the graphs in Fig. 8a and Fig. 8b that the beachhead spatio-temporal dynamics appears in the problem when the road width is $\delta \in [\delta_1, \delta_2]$. The left boundary δ_1 is shown in the graph $c(\delta)$ in Fig. 8a. It can be defined as the minimum road width that prevents further propagation of the population wave, *i.e.,* $c(\delta_1) = 0$ and $c(\delta) > 0$ for any $0 < \delta < \delta_1$. The right boundary δ_2 is shown in the graph $W(\delta)$ in Fig. 8b, where it is identified as the minimum road width that results in the population extinction in front of the road, *i.e.,* $W(\delta) = 0$ for any $\delta \geqslant \delta_2$. We note that, for a given road width δ, the width and height of the beachhead depend on the parameters A and ρ of the growth function; see Fig. 9. The parameter range (ρ, A) required for formation of the beachhead spatial domain is shown for a given road width in Fig. 10.

Let us fix A in the definition of the growth function (5) and vary another demographic parameter ρ in (5) and the road width δ. Based on the analysis above, we anticipate having several regions in the (ρ,δ)-plane that correspond to various spatio-temporal dynamics regimes and we aim to find boundaries $\delta = \delta(\rho)$ between those regions and identify the critical road width required for the beachhead regime.

The curve that separates the extinction region in the (ρ,δ)-plane from the other regimes is defined directly from the analysis of the growth function (5), *i.e.,* we require that the population density behind the road is given by the stable steady state $\bar{N}_3$ in (7) which only exists when $\rho \geqslant 2\sqrt{A}$. Thus, we define a boundary B_1 of the extinction region in the parametric plane as $B_1 : \rho = 2\sqrt{A}$ for all values of δ. The straight line B_1 is shown in Fig. 11a where it separates the extinction region I from the other regimes.

Consider now $\rho > 2\sqrt{A}$ and let the population density brought to the front of the road from behind the road be below the threshold density ϵ. It follows from our discussion of the logistic growth function (2) in the previous section, that the invasive species will not spread in front of the road, *i.e.,* we have the barrier regime. The boundary B_2 of the barrier region is given by the same condition (28) as for the logistic growth function. For the growth function (5), the condition (28) written at the stable steady state $\bar{N}_3$ becomes

$$\frac{\rho + \sqrt{\rho^2 - 4A}}{2}\phi(\delta) = \epsilon,$$

which we can rearrange for ρ to give the equation of the boundary curve B_2 in the parametric plane,

$$B_2 : \rho = \frac{A\phi^2(\delta) + \epsilon^2}{\phi(\delta)\epsilon}. \tag{30}$$

The curve B_2 shown in Fig. 11 bounds the region *II* which corresponds to the barrier regime in the spatial domain.

Let us now investigate the beachhead regime where the population density brought to the region in front of the road is fully compensated by the negative growth at the demographic stage. In our further analysis, we approximate the beachhead case by the following condition

$$N_{t+1}(b+\delta) = N_t(b+\delta), \text{ for } \epsilon < N < \bar{N}_2, \tag{31}$$

i.e., we require that the population density remains constant at the edge of the road in the beachhead regime.

The population density at time $t+1$ can be presented as

$$N_{t+1} = N_t + \Delta N,$$

where the increment ΔN is brought to the edge of the road over the dispersal stage. Since the travelling wave given by (21) has the constant height h behind the road, the increment ΔN in the population density remains constant at any time t for a given road width $\delta > 0$, yet its value depends on δ; see the discussion in Section 3.1. This increment is then compensated by the negative growth occurred when $\epsilon < N < \bar{N}_2$ at the growth stage to meet the condition (31).

It follows from the above consideration that the beachhead regime is entirely related to the Allee effect, *i.e.,* the negative growth at the interval $N \in [\epsilon, \bar{N}_2]$. This conclusion is further illustrated in Fig. 12 where the growth function $F(N)$ given by (5) is

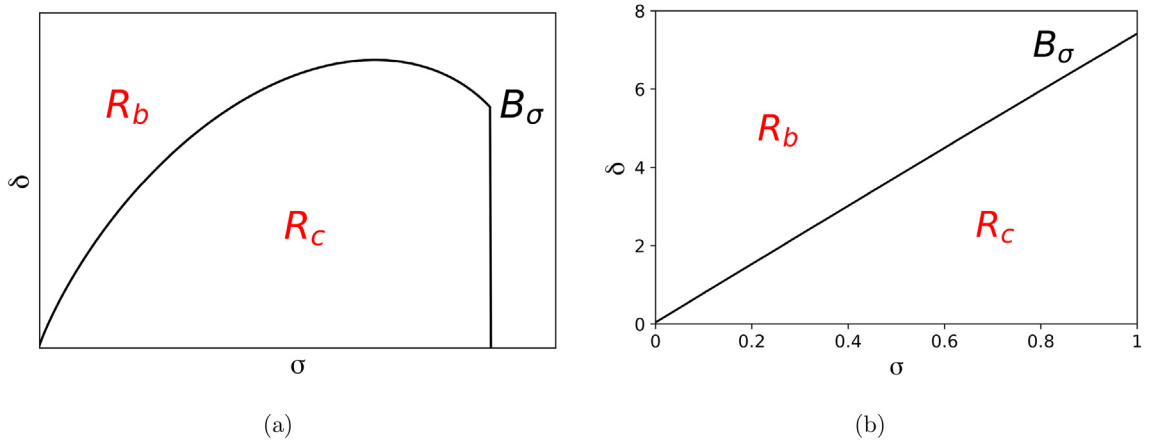

Fig. 6. The propagation regimes in the road model (14)-(18) with the growth function (2) shown in the (σ, δ)-plane. The region R_c represents the corridor regime in the spatial domain, the region R_b represents the barrier regime. (a) The boundary B_σ between regions R_b and R_c determines the critical width of the road δ_b required to stop propagation of the invasive species for any given value of the parameter σ in the dispersal kernel (10); see further explanation in the text. (b) The boundary B_σ shown for $\sigma \in [0, 1]$. The boundary curve can be approximated by a linear function $B_\sigma : \delta = \kappa\sigma$, where the slope of the straight line has been computed as $\kappa \approx 7.38$ for $\epsilon = 10^{-7}$ and $A = 3$.

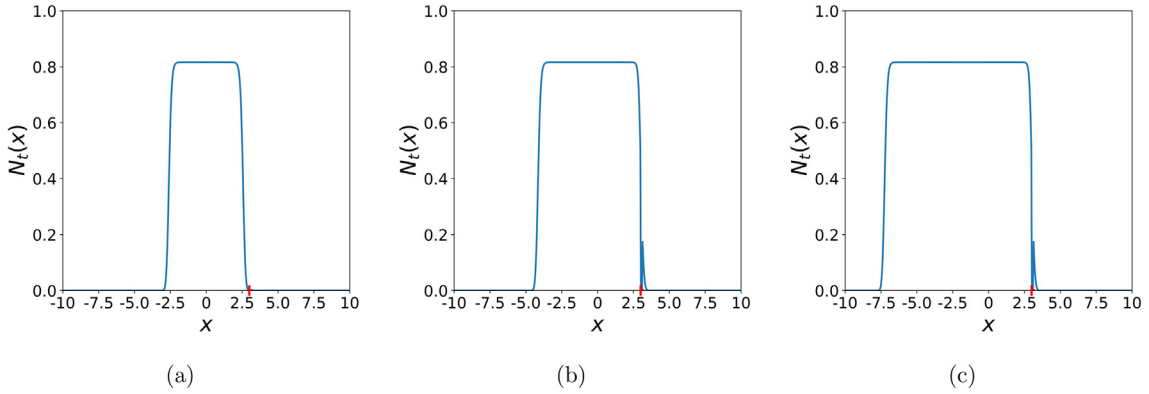

Fig. 7. The beachhead regime in the problem (14)-(18) with the growth function (5). The parameters are $A = 0.15, \rho = 1.0$. The road width is $\delta = 0.12$ and the road region is shown in red on the x-axis. (a) A travelling wave approaches the road at time $t = 50$, (b) The population density distribution $N_t(x)$ at time $t = 100$. The beachhead region in front of the road has been invaded, yet the invasive species does not propagate further into the space, (c) The population density distribution $N_t(x)$ in front of the road remains the same at time $t = 200$ as in earlier times (cf. Fig. 7b).

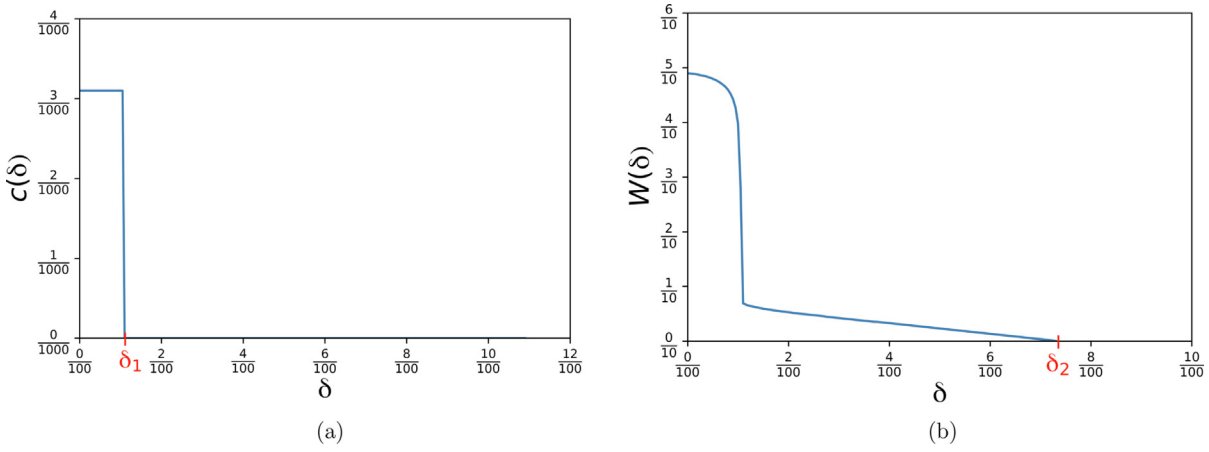

Fig. 8. The problem (14)-(18) with the growth function (5). The rate of spread c and width W of the domain occupied by the population in front of the road are shown as functions of the road width δ measured as percentage of the domain size L. The parameters are $A = 0.15, \rho = 1.0$. (a) For any road width $\delta > \delta_1$, the population does not spread in front of the beachhead region. (b) For any road width $\delta > \delta_2$, the road acts as a barrier that the invasive population cannot cross.

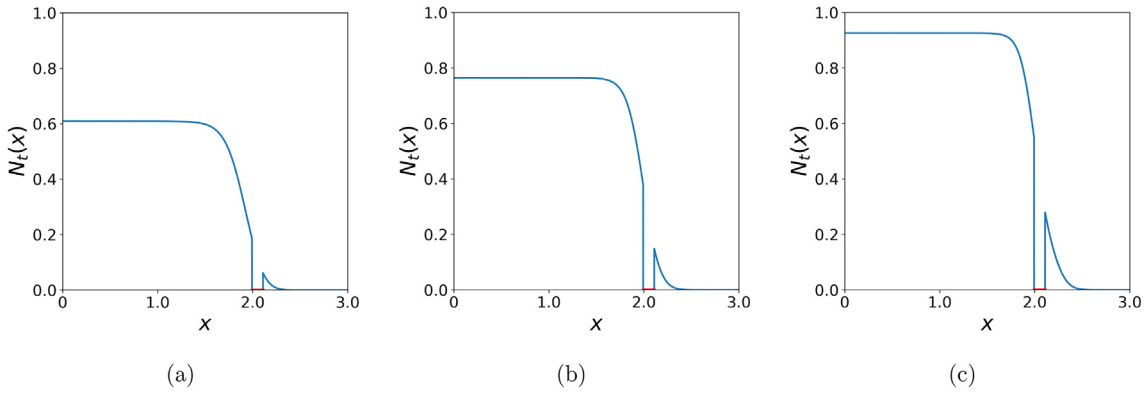

Fig. 9. The population density distributions $N_t(x)$ at time $t = 300$ after the beachhead region has been invaded in front of the road. For the given road width $\delta = 0.12$, the size of the beachhead region depends on the parameters of the growth function (5). (a) The parameters are $A = 0.15, \rho = 0.855$, (b) $A = 0.18, \rho = 1.0$, (c) $A = 0.18, \rho = 1.12$. Only the spatial subdomain $x \in [0, 3]$ is shown in the figure for the sake of better visualisation of the beachhead region.

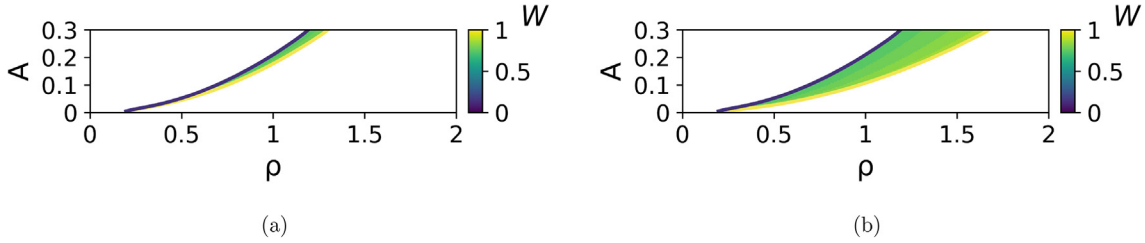

Fig. 10. The spatial width of the beachhead region W as a function of the parameters ρ and A in the growth function (5). (a) The road width is $\delta = 0.12$, (b) the road width is $\delta = 0.19$.

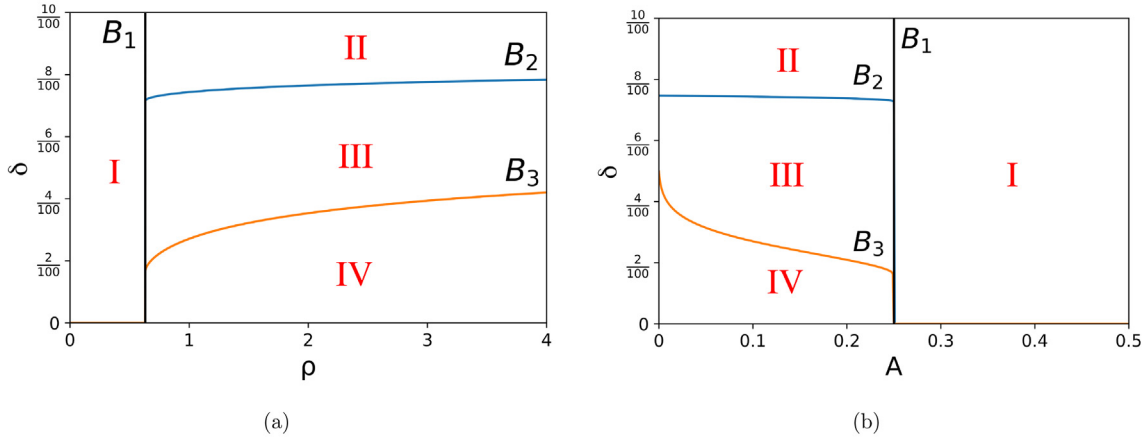

Fig. 11. Various spatio-temporal dynamics regimes in the road model (14)-(18) with the growth function (5). (a) The parametric plane (ρ, δ). Region *I* represents the extinction regime in the spatial domain. Region *II* is the barrier regime, where the road prevents propagation of the invasive species. Region *III* is the beachhead regime, where the population invades a spatial beachhead region in front of the road without further propagation. Region *IV* is the corridor regime, where the invasive population crosses the road and a travelling wave spreads in front of the road to invade the entire domain as time progresses. (b) The parametric plane (A, δ). The notation used to mark different regions is the same as in Fig. 11a.

shown as a black solid line and a dashed line is the equilibrium line $F(N) = N$. Let us draw a new growth function $F(N) + \Delta N$, where $\Delta N = const$, *i.e.,* we move the graph of the function $F(N)$ along the y-axis by the distance ΔN. For relatively small ΔN, this transformation results in a new stable steady state, *i.e.,* formation of the beachhead regime; see curve A in the figure, where $\Delta N_1 < \Delta N_{cr}$ and the new stable steady state is shown as a blue dot on the line $F(N) = N$. As ΔN increases, the new steady state defining the beachhead regime moves closer to the steady state $\overline{N}_2$ along the equilibrium line $F(N) = N$, and the two steady states coincide when $\Delta N = \Delta N_{cr}$ (curve B in the figure). For any $\Delta N_2 > \Delta N_{cr}$, we have the corridor regime only, as $F(N) + \Delta N > N$ and the population grows in front of the road (curve C).

The increment ΔN_{cr} defines the transformation of the beachhead regime to the corridor regime. Since ΔN depends on the road width, $\Delta N = \Delta N(\delta)$, the boundary B_3 between the beachhead region and the corridor region in the parametric plane (ρ, δ) can be found from the condition

$$F(N^*) + \Delta N_{cr}(\delta) = N^*, \tag{32}$$

where N^* is defined from the requirement that the line $F(N) = N$ is the tangent line for the function $F(N) + \Delta N$ at point N^*, *i.e.,* we have

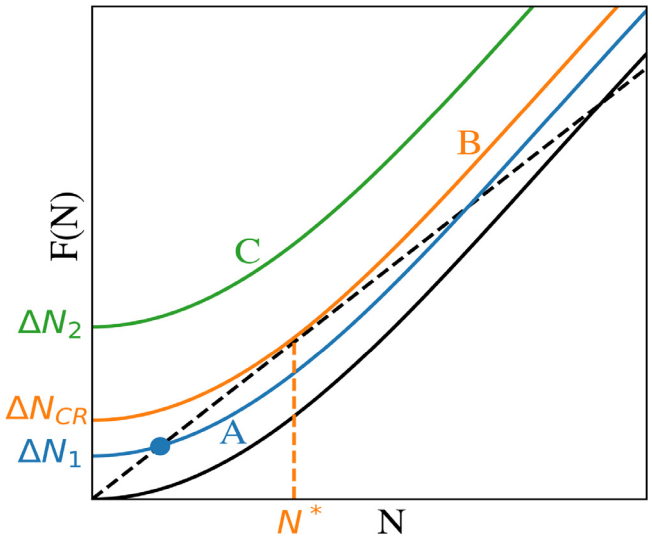

Fig. 12. The beachhead regime is produced by the Allee effect. The original Allee growth function (5) (black solid line) has the only point of intersection $N = \bar{N}_2$ with the line $F(N) = N$ (dashed line) in the interval $N \in [\epsilon, \bar{N}_2]$. Another point of intersection appears when $F(N)$ is raised by the value $\Delta N < \Delta N_{cr}$ (curve A, blue solid line). The new stable steady state shown as a blue dot in the figure corresponds to the beachhead distribution of the population density in the spatial domain. As ΔN increases, the new steady state goes up along the line $F(N) = N$, while the unstable steady state $\bar{N}_2$ goes down along the curve. At $\Delta N = \Delta N_{cr}$, the beachhead steady state coincides with the unstable steady state; see curve B (orange solid line) in the figure. For any $\Delta N > \Delta N_{cr}$, the condition $F(N) + \Delta N > N$ holds and provides the corridor regime (curve C, green solid line).

$F'(N) = 1$ at $N = N^*$. Differentiating $F(N)$ and rearranging terms we arrive at

$$N^4 + 2AN^2 - 2A\rho N + A^2 = 0, \tag{33}$$

where we require $\rho > 2\sqrt{A}$ and $\epsilon < N < \bar{N}_2$. Let us fix the parameter A in the growth function (5). The Eqs. (33) and (32) are then solved for any given value of ρ to find the curve $\delta = \delta(\rho)$. The boundary $B_3 : \delta = \delta(\rho)$ is shown in Fig. 11.

The position of the boundary curves in the parametric plane is defined by parameters in (30) and (32). Consider, for example, the boundary B_2 shown in Fig. 13a, where the curve B_2 is defined from (30) for some baseline value of the threshold density $\epsilon = \epsilon^*$. The boundary B_2 will move down to make the barrier region larger and the beachhead region more narrow when ϵ increases to $\epsilon^{**} > \epsilon^*$; see a dash-dotted line in Fig. 13a. Furthermore, it follows from the analysis in Fig. 12 that the beachhead region between the boundaries B_2 and B_3 will completely disappear in the extreme case $\epsilon > N^*$, where N^* is defined by (33). Conversely, the boundary B_2 will move up to decrease the size of the barrier region when ϵ decreases to some $\epsilon^{***} < \epsilon^*$ (see a dashed line in Fig. 13a). It also follows from (6) and (32) that the boundaries B_1 and B_3 do not move when we vary the threshold density ϵ.

Consider now the boundary B_3 that corresponds to the baseline value of the demographic parameter $A = A^*$ as shown in Fig. 13b. Let us decrease A to some new value $A^{**} < A^*$. The boundary B_1 will move to the left when A decreases, while the boundary B_3 will move up to increase the size of the corridor domain in the parametric plane (see dash-dotted lines in the figure). Conversely, let the new parameter value be $A^{***} > A^*$. It can be seen from Fig. 13b that the corridor domain will shrink as the boundary B_1 moves to the right and the boundary B_3 moves down (see dashed lines in the figure). These conclusions are similar to the case of the logistic growth: if environmental conditions become harsher in front of the road, a more narrow road will be able to prevent propagation of the invasive species.

4. Conclusions

In the present paper, we have developed a novel model that allows one to take into account different dispersal and growth behaviour of invasive plant species when a road is presented in a spatial domain. A stage-structured population has been considered in the model where the condition of no growth in the road sub-domain has been implemented at the growth stage, and the dispersal stage has included sweeping the population from the road.

The aim of our investigation has been to understand whether roads can always be thought of as corridors to facilitate propagation of the invasive species. The rate of spatial spread of the alien species is a quantity of high theoretical and practical importance, and it has been a focus of numerous studies (Andow et al., 1990; Clark et al., 2001; Fisher, 1937; Hastings et al., 2005; Kot et al., 1996; Lewis and Pacala, 2000). The rate of spread is known to depend strongly on the dispersal mode, so that the short-distance dispersal normally results in the advance with a constant speed, but the long-distance dispersal (described by a fat-tailed kernel with a power-law decay) may lead to a spread with accelerating speed (Kot et al., 1996). The results we have obtained in the 1-D spatial road model demonstrate that, in the case of the short-distance dispersal, the growth function is a dominant factor responsible for propagation of invasive species in front of the road. Depending on the parameters of the growth function, invasion into space may not be prevented by the road, yet the same road may serve as a barrier stopping the spread of the invasive species. The logistic growth function results in the corridor propagation regime where the population advances at a constant speed in front of the road and the barrier regime where no population exist in front of the road. Those regimes are defined by the road width δ, and there exists a threshold value of δ for which the barrier regime turns into the corridor regime to result in propagation of the invasive species in front of the road. It has been explained in the paper how the threshold width of the road depends on the growth parameter A in the definition of the logistic growth function.

Meanwhile, between the two growth functions we have investigated in the paper, the growth with the Allee effect results in more complex conditions of propagation in comparison with the logistic growth. We have observed a beachhead propagation regime when the growth function with the Allee effect has been employed in the problem. In the latter case the population remains constant in front of the road and does not spread into space in front of the road as time progresses. The beachhead phenomenon investigated in the paper is similar to invasion pinning (see Keitt et al., 2001 and references therein). It has been shown in Keitt et al. (2001) that the Allee growth function can be responsible for invasion pinning in the system with discrete space, and our results further demonstrate the importance of the Allee effect in spatially continuous models where spatial heterogeneity is present in the landscape. Analysis of the parameters in the problem revealed that the beachhead regime can be considered as the transition between the corridor and barrier regimes. It has been argued in the paper that a small change in conditions of the environment favouring the invasive species, for example, due to climate change, can change the propagation regime, allowing the invasive species to invade the domain in front of the road where it previously could not spread.

The results we present in the paper have been obtained in a simple 1-D layout. In the 1-D problem, the 'road' can be thought

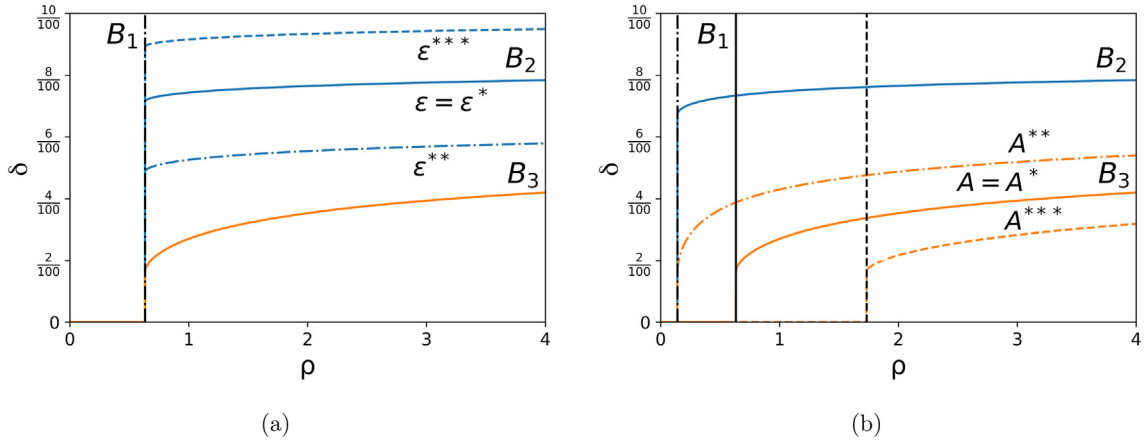

Fig. 13. The Allee growth function (5): domains in the parametric plane (ρ, δ) corresponding to different spatio-temporal dynamics regimes when problem parameters are varied. (a) The size of the barrier domain defined by the position of the boundary B_2 increases when the value of the threshold density ϵ increases from ϵ^* (the solid line B_2 in the figure) to $\epsilon^{**} > \epsilon^*$; a new position of the boundary B_2 is shown as a dash-dotted line in the figure. Conversely,the size of the barrier domain decreases when the threshold density ϵ decreases from ϵ^* to $\epsilon^{***} < \epsilon^*$ (a dashed line in the figure). (b) The size of the corridor domain defined by the position of the boundaries B_1 and B_3 increases when the value of the demographic parameter A decreases from A^* (the solid lines B_1 and B_3 in the figure) to $A^{**} < A^*$; new boundaries B_1 and B_3 are shown as dash-dotted lines in the figure. Conversely, the size of the corridor domain decreases when the value of A increases from A^* to $A^{***} > A^*$ (dashed lines in the figure).

of as an open space in the fragmented forest landscape where the conditions of growth are essentially different from the rest of the spatial domain. Meanwhile, we expect that the model we have considered can serve as a framework for a more realistic model employed to study invasion in 2-D spatial domains. We notice that in the case of the Gaussian dispersal kernel (10), the 2-D dispersal in the isotropic environment is given by a product of two 1-D dispersal kernels simulating dispersal in the x- and y-directions. Hence, in an isotropic environment, an intuitive extension of our results onto the 2-D case is straightforward, and depending on the parameters of the growth function, one can expect the same propagation regimes as obtained in our 1-D model. These properties, however, may change if the 2-D environment becomes anisotropic, e.g., if propagation of the invasive species along the road is much faster than in the direction orthogonal to the road. The latter condition leads to the requirement of incorporation of long-distance dispersal into the model, as this type of dispersal is indeed the primary dispersal type for many invasive plants (Kot et al., 1996; Nathan et al., 2011; Straigytė et al., 2015; Thuiller et al., 2006). Since the 2-D framework allows for more realistic modelling, natural seed dispersal in the direction orthogonal to the road (as given by the Gaussian dispersal kernel in the 1-D model) will be complemented by dispersal through wind along the road simulated by a different dispersal kernel. While our model is flexible enough to deal with directional 2-D dispersal, the analysis of long-distance dispersal is a more challenging issue, both from a mathematical and computational viewpoint, and is reserved as a topic of future work. Another possible direction of future research is incorporation of seed banks into the model to take into account seeds that may lie dormant for some time before germinating (MacDonald and Watkinson, 1981). Integro-difference models have been used successfully for study of populations with a fraction of non-germinating seeds (Allen et al., 1996; Li, 2012; Mistro et al., 2005) and combining the concepts of a seed bank and a heterogeneous landscape in the model may contribute to better understanding of invasive scenarios. Finally, we would be interested in more thorough investigation of the growing conditions at road edges to understand how they may facilitate the spread of invasive plant species (Hansen and Clevenger, 2005) beyond the area adjacent to the road. The study of this topic may require a more sophisticated definition of the growth function in our model and we leave it for future work.

CRediT authorship contribution statement

Bradly Deeley: Methodology, Software, Validation, Investigation, Visualization, Writing - original draft, Writing - review & editing. **Natalia Petrovskaya:** Conceptualization, Methodology, Investigation, Writing - original draft, Writing - review & editing, Supervision.

Declaration of Competing Interest

The authors declare that they have no known competing financial interests or personal relationships that could have appeared to influence the work reported in this paper.

Acknowledgments

B.F.D. acknowledges support in the form of a Forest Edge Fellowship from the Leverhulme Trust and University of Birmingham.

Appendix A. The increment in the population density in front of the road

We consider the approximation of (22) used to analyse various propagation regimes in front of the road. While the calculation of the $N_{t+\frac{1}{2}}(x)$ term in (22) is straightforward, the calculation of the second term, $N^R_{t+1}(x)$, is more complicated. It has been shown in Section 3.1 that additional dispersal of the population density $N^R_{t+1}(x)$ across the road is given by

$$N^R_{t+1}(x) = F(h)\frac{1}{2}\int_b^{b+\delta}\left(\operatorname{erf}\left(\frac{b-y}{\sigma\sqrt{2}}\right)+\operatorname{erf}\left(\frac{y-a}{\sigma\sqrt{2}}\right)\right) \times\left(\frac{1}{\sqrt{2\pi\sigma^2}}\exp\left(\frac{-|x-y|^2}{2\sigma^2}\right)\right)dy. \tag{34}$$

Since we cannot calculate the integral in (34) analytically, we use the following approximation of the error function $\operatorname{erf}(x)$ introduced in Tsay et al. (2013) which is valid for $x \geqslant 0$,

$$\operatorname{erf}(x) \approx 1 - \exp\left(c_1 x + c_2 x^2\right), \tag{35}$$

where the coefficients c_1 and c_2 have been evaluated in Tsay et al. (2013) as $c_1 = -1.09599814703333$, and $c_2 = -0.75651138383854$.

Substituting this approximation into (34) and rearranging terms we arrive at

$$\begin{aligned} N_{t+1}^{R}(x) &= F(h)\frac{1}{2}\int_{b}^{b+\delta}\left(\operatorname{erf}\left(\frac{b-y}{\sigma\sqrt{2}}\right)\right. \\ &\quad \left.+\operatorname{erf}\left(\frac{y-a}{\sigma\sqrt{2}}\right)\right)\left(\frac{1}{\sqrt{2\pi\sigma^2}}\exp\left(\frac{-|x-y|^2}{2\sigma^2}\right)\right)dy \\ &= F(h)\frac{1}{2}\frac{1}{\sqrt{2\pi\sigma^2}}\int_{b}^{b+\gamma}\left(\exp\left(-d_1y^2+d_2y+d_3\right)\right. \\ &\quad \left.-\exp\left(-d_1y^2+d_4y+d_5\right)\right)dy, \end{aligned} \tag{36}$$

where the coefficients $d_i, i = 1,\ldots,5$ are defined as follows:

$$\begin{aligned} d_1 &= -\left(\frac{c_2-1}{2\sigma^2}\right), d_2 = \left(\frac{2x+\sqrt{2}\sigma c_1-2c_2b}{2\sigma^2}\right), \\ d_3 &= \left(\frac{-\sqrt{2}\sigma c_1b+c_2b^2-x^2}{2\sigma^2}\right), \\ d_4 &= \left(\frac{2x+\sqrt{2}\sigma c_1-2ac_2}{2\sigma^2}\right), \\ d_5 &= \left(\frac{-\sqrt{2}\sigma ac_1+a^2c_2-x^2}{2\sigma^2}\right). \end{aligned} \tag{37}$$

References

Allen, E.J., Allen, L.J.S., Gilliam, X., 1996. Dispersal and competition models for plants. J. Math. Biol. 34, 455–481.

Andersen, M., 1991. Properties of some density-dependent integrodifference equation population models. Math. Biosci. 104, 135–157.

Andow, D.A., Kareiva, P.M., Levin, S.A., Okubo, A., 1990. Spread of invading organisms. Landscape Ecol. 4, 177–188.

Boukal, D.S., Berec, L., 2002. Single-species models of the Allee effect: extinction boundaries, sex ratios and mate encounters. J. Theor. Biol. 218 (3), 375–394.

Clark, J.S., Lewis, M.A., Horvath, L., 2001. Invasion by extremes: population spread with variation in dispersal and reproduction. Am. Nat. 157, 537–554.

Damschen, E.I. et al., 2014. How fragmentation and corridors affect wind dynamics and seed dispersal in open habitats. PNAS 111 (9), 3484–3489.

Essl, F., Milasowszky, N., Dirnbck, T., 2011. Plant invasions in temperate forests: resistance or ephemeral phenomenon? Basic Appl. Ecol. 12 (1), 1–9.

Fisher, R., 1937. The wave of advance of advantageous genes. Ann. Eugenics 7, 355–369.

Forman, R.T.T., Sperling, D., Bissonette, J.A., Clevenger, A.P., Cutshall, C.D., Dale, V.H., Fahrig, L., France, R., Goldman, C.R., Heanue, K., Jones, J.A., Swanson, F.J., Turrentine, T., Winter, T.C., 2002. Road Ecology: Science and Solutions. Island Press, Washington, DC, USA.

Gilbert-Norton, L., Wilson, R., Stevens, J.R., Beard, K.H., 2010. A meta-analytic review of corridor effectiveness. Conserv. Biol. 24 (3), 660–668.

Haddad, N.M., Bowne, D.R., Cunningham, A., Danielson, B.J., Levey, D.J., Sargent, S., Spira, T., 2003. Corridor use by diverse taxa. Ecology 84 (3), 609–615.

Hansen, M.J., Clevenger, A.P., 2005. The influence of disturbance and habitat on the presence of non-native plant species along transport corridors. Biol. Conserv. 125, 249–259.

Hastings, A., Cuddington, K., Davies, K.F., Dugaw, C.J., Elmendorf, S., Freestone, A., Harrison, S., Holland, M., Lambrinos, J., Malvadkar, U., Melbourne, B.A., 2005. The spatial spread of invasions: new developments in theory and evidence. Ecol Lett. 8, 91–101.

Holmes, T.P., Aukema, J.E., Von Holle, B., Liebhold, A., Sills, E., 2009. Economic impacts of invasive species in forests. Ann. N. Y. Acad. Sci. 1162, 18–38.

Keitt, T.H., Lewis, M.A., Holt, R.D., 2001. Allee effects, invasion pinning, and species' borders. Am. Nat. 157, 203–216.

Kot, M., Schaffer, W.M., 1986. Discrete-time growth-dispersal models. Math. Biosci. 80, 109–136.

Kot, M., Lewis, M.A., van der Driessche, P., 1996. Dispersal data and the spread of invading organisms. Ecology 77, 2027–2042.

Langmaier, M., Lapin, K., 2020. A systematic review of the impact of invasive alien plants on forest regeneration in European temperate forests. Front. Plant Sci. 11, 1349.

Lewis, M.A., Pacala, S., 2000. Modeling and analysis of stochastic invasion processes. J. Math. Biol. 41, 387–429.

Lewis, M.A., Petrovskii, S.V., Potts, J., 2016. The Mathematics Behind Biological Invasions. Interdiscip. Appl. Math. 44, Springer.

Li, B., 2012. Traveling wave solutions in a plant population model with a seed bank. J. Math. Biol. 65, 855–873.

MacDonald, N., Watkinson, A.R., 1981. Models of an annual plant population with a seedbank. J. Theor. Biol. 93, 643–653.

Mistro, D.C., Rodrigues, L.A.D., Schmid, A., 2005. A mathematical model for dispersal of an annual plant population with a seed bank. Ecol. Model. 188, 52–61.

Mortensen, D.A., Rauschert, E.S.J., Nord, A.N., Jones, B.P., 2009. Forest roads facilitate the spread of invasive plants. Invasive Plant Sci. Manage. 2, 191–199.

Musgrave, J., Girard, A., Lutscher, F., 2015. Population spread in patchy landscapes under a strong Allee effect. Theor. Ecol. 8, 313–326.

Nathan, R., Katul, G.G., Bohrer, G., Kuparinen, A., Soons, M.B., Thompson, S.E., Trakhtenbrot, A., Horn, H.S., 2011. Mechanistic models of seed dispersal by wind. Theor. Ecol. 4 (2), 113–132.

O'Reilly-Nugent, A., Palit, R., Lopez-Aldana, A., et al., 2016. Landscape effects on the spread of invasive species. Curr. Landscape Ecol. Rep. 1, 107–114.

Pimentel, D., Lach, L., Zuniga, R., D. Morrison, D. (2000) Environmental and economic costs of non-indigenous species in the United States. BioScience, 50 (1): 53–65.

Rodrigues, L.A.D., Mistro, D.C., Cara, E.R., Petrovskaya, N.B., Petrovskii, S.V., 2015. Patchy invasion of stage-structured alien species with short-distance and long-distance dispersal. Bull. Math. Biol. 77, 1583–1619.

Sala, O.E. et al., 2000. Global biodiversity scenarios for the year 2100. Science 287 (5459), 1770–1774.

Sanderson, L.A., McLaughlin, J.A., Antunes, P.M., 2012. The last great forest: A review of the status of invasive species in the North American boreal forest. Forestry 85 (3), 329–340.

Straigytė, L., Cekstere, G., Laivins, M., Marozas, V., 2015. The spread, intensity and invasiveness of the Acer negundo in Riga and Kaunas. Dendrobiology 74, 157–168.

Thuiller, W., Richardson, D.M., Rouget, M., Proches, S., Wilson, R.U., 2006. Interactions between environment, species traits, and human uses describe patterns of plant invasions. Ecology 87, 1755–1769.

Travers, E., Härdtle, W., Matthies, D., 2021. Corridors as a tool for linking habitats – Shortcomings and perspectives for plant conservation. J. Nat. Conserv. 60, 125974.

Tsay, W.-J., Huang, C.J., Fu, T.-T., Ho, I.-L., 2013. A simple closed-form approximation for the cumulative distribution function of the composite error of stochastic frontier models. J. Productivity Anal. 39, 259–269.

Tyser, R.W., Worley, C.A., 1992. Alien flora in grasslands adjacent to road and trail corridors in Glacier National Park, Montana (USA). Conserv. Biol. 6, 253–262.

Vilà, M., Ibáñez, I., 2011. Plant invasions in the landscape. Landscape Ecol. 26, 461–472.